Journal of Nuclear Materials 385 (2009) 431–434

Contents lists available at ScienceDirect

Journal of Nuclear Materials

journal homepage: www.elsevier.com/locate/jnucmat

Thermal behaviour of cesium implanted in cubic zirconia

L. Vincent *, L. Thomé, F. Garrido, O. Kaitasov

CSNSM-UMR8609, CNRS-IN2P3-Université Paris-Sud, F-91405 Orsay-Campus, France

ARTICLE INFO

PACS:
61.80.−x
61.72.U−
61.82.Ms
61.72.Ff
61.72.sh
68.37.Lp

ABSTRACT

Cesium ions were implanted at the energy of 300 keV in YSZ at 300 and 1025 K, with increasing fluences up to 5×10^{16} cm^{-2}. Concentration profiles were determined by Rutherford Backscattering Spectrometry (RBS) measurements. Transmission Electron Microscopy (TEM) experiments were achieved to determine the nature of the damages and to characterize a predicted ternary phase of cesium zirconate. At 300 K, amorphization occurs at high Cs-concentration (9 at.%) due to a chemical effect. TEM investigations performed after *in situ* post-annealing shows the recrystallization of YSZ concurrently with the cesium release. No precipitation of secondary phases was observed after annealing. With implantation performed at 1025 K, dislocation loops and bubbles were formed but the structure did not undergo amorphization. Dislocation rearrangement leads to the polygonization of the matrix. The cesium concentration reaches a saturation value of 1.5 at.%, and once more no precipitation is observed.

© 2008 Elsevier B.V. All rights reserved.

1. Introduction

Plutonia doped cubic zirconia is foreseen to be used in light water reactors as an inert matrix fuel for actinide transmutation [1,2]. For this application, the main criteria are: radiation resistance, phase stability, chemical inertness and insolubility after irradiation. Another crucial issue is the ability of the matrix to confine radiotoxic fission products. This issue has received only few attentions, especially concerning the retention of Cs at high temperature. Pouchon et al. [3] have calculated the solubility limit of Cs to be 1.5 at.% at 2000 K, whereas Wang et al. [4] have estimated that the defective implanted matrix could accept a higher concentration of Cs up to 8 at.% at room temperature. Nevertheless, the inner operating temperature of inert matrix fuels in reactors is likely to reach 1900 K [5,6]. In those conditions Cs diffusion, release and/or precipitation are expected.

The precipitation of cesium zirconate (Cs_2ZrO_3) was predicted by numerous authors [3,7,8]. Hence, the solubility and retention of Cs in cubic zirconia was studied at high temperature. The purpose of the present work was to determine experimentally the phase in which Cs is fixed in Yttria Stabilized Zirconia (YSZ), i.e. solid solution or cesium zirconate precipitates. It has been performed by using the ion implantation technique to incorporate Cs species into YSZ single crystals, at room temperature (RT) and at a temperature of 1025 K (HT). Previous transmission electron microscopy (TEM) observations on Cs-implanted YSZ [9,10] demonstrated the formation of nanometer-sized domains at low fluence up to 10^{15} cm^{-2}. These distorted areas induce large strain fields, causing the formation of misfit dislocations. These domains are also observed on Xe-implanted YSZ and are thus considered to be due to a ballistic effect during implantation. Moreover, Rutherford Backscattering Spectrometry and Channeling (RBS/C) and TEM experiments [9] indicate that the damage build-up and the nature of defects depend on the implantation temperature. At 1300 K dislocation loops are formed instead of nanodomains. TEM micrographs do not reveal the formation of any secondary phase for both implantation temperatures up to 10^{16} cm^{-2} (this fluence corresponds to a concentration of 1.8 at.% which is about the value of solubility estimated by Pouchon et al. [3]). Here additional TEM experiments have been carried out to observe the possible formation of Cs precipitates at high fluence (up to 5×10^{16} cm^{-2}) and to determine the nature of the damage created by implantation. Thermal annealings up to 1025 K were performed on RT-implanted samples to compare the recovered structure with the damaged structure after implantation at 1025 K. Concentration profiles were also recorded at increasing fluences by RBS.

2. Experimental

The specimen used in the present study are YSZ single crystals (<1 0 0> orientation) containing 9.5 mol% Y_2O_3, synthesized by the Crystal-GmbH company. All samples were coated with a conductive carbon layer (thickness adapted to the characterization technique) to avoid charge effects under ion or electron beams.

Bulk samples were implanted at RT and 1025 K with increasing fluences of Cs up to 5×10^{16} cm^{-2}. The Cs^{2+} ion energy was 300 keV, leading to a projected range of about 67 nm. The depth

* Corresponding author. Tel.: +33 1 69 15 52 31; fax: +33 1 69 15 52 68.
E-mail address: laetitia.vincent@csnsm.in2p3.fr (L. Vincent).

0022-3115/$ - see front matter © 2008 Elsevier B.V. All rights reserved.
doi:10.1016/j.jnucmat.2008.12.013

distribution of implanted species was estimated using the SRIM code [11].

RBS analyses were carried out *in situ* with the JANNUS facility of the CSNSM in Orsay [12]. After each implantation step, RBS measurements were performed at temperature near RT with a 3.065 MeV He^{2+} beam. The energy resolution of the electronic set-up was 15 keV, corresponding to a depth resolution of the order of 10 nm in YSZ.

Samples implanted at 5×10^{16} cm^{-2} were cut and thinned for cross-sectional transmission electron microscopy (XTEM) examinations using a Tecnai G20 operating at 200 keV. The thermal evolution of RT-implanted XTEM samples was performed *in situ* by successive isochronal annealing for 15 min from 575 to 1025 K. A final annealing was performed at 1025 K for 1 h.

3. Results

Bright-field TEM micrograph recorded on the cross-section of a sample implanted at RT is shown in Fig. 1. At high fluence (5×10^{16} cm^{-2}), Cs ion implantation leads to an amorphous layer between two damaged zones. The amorphous nature is confirmed by the presence of a diffuse ring in the selected area electron diffraction (SAED) pattern (Fig. 2). No secondary crystalline phase is observed. The radius of the ring corresponds to a distance $d = 3$ Å in the real space which according to the Guinier formula [13], can be related to an average nearest-neighbour distance $x = 3.7$ Å in the amorphous material. This value is slightly higher than the

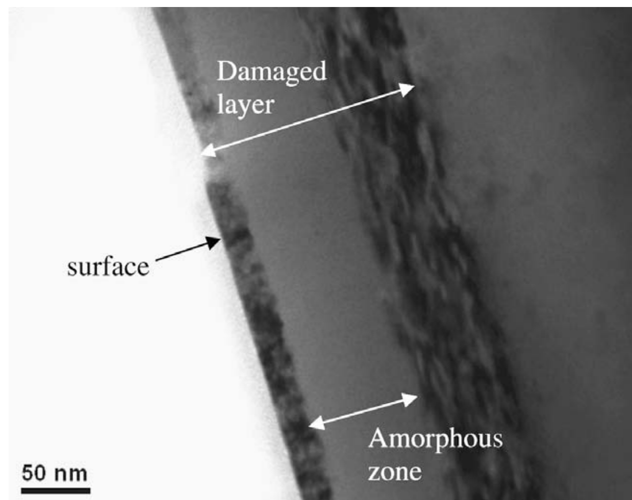

Fig. 1. Bright-field TEM micrograph of the cross-section of YSZ implanted with 300 keV Cs ions at RT with a fluence of 5×10^{16} cm^{-2}.

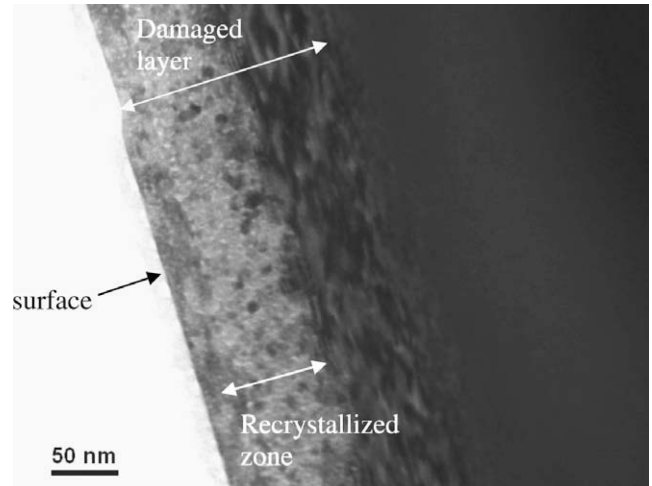

Fig. 3. TEM micrograph of YSZ implanted with 300-keV Cs ions (5×10^{16} cm^{-2}) and annealed at 1025 K during 1 h. Recrystallization occurs by the formation of rounded nanocrystals in the previous amorphized layer (see Fig. 1).

lowest interatomic distance in the cubic ZrO_2 crystal (3.6 Å) meaning that the amorphization is accompanied by a weak swelling.

Thermal treatments of implanted samples have been performed up to 1025 K in order to follow the thermodynamic evolution of the amorphous layer and to identify the phases formed upon Cs diffusion. Annealing was carried out *in situ* on XTEM samples. The temperature was raised stepwise with 375 K intervals from 575 to 1025 K. The evolution of SAED patterns as a function of the annealing temperature is presented in Fig. 2. As discuss previously, as-implanted samples show a characteristic amorphous ring. At 575 K, any noticeable change of the diffuse rings was observed. At 775 K the intensity of the diffuse ring decreases indicating a partial recrystallization which becomes significant above 675 K. At this temperature the appearance of new spots was observed. They are randomly positioned on rings whose d_{hkl} corresponds to cubic ZrO_2, in particular (111), (200), (220) and (311). Thus, a non-epitaxial recrystallization of the amorphous layer occurs during annealing. The recrystallized layer is imaged on Fig. 3. The micrograph recorded in bright-field conditions shows rounded crystallites in the previously amorphized zone. Following the temperature rise up to 1025 K, an increase of the number and of the size of recrystallized areas was observed. It is worth noting that no secondary phase could be observed after this annealing.

Also implantations have been performed at 1025 K. Previously it has been demonstrated that the damage is clearly dependent on the implantation temperature [9]. At 1025 K, point defects coalesce to form dislocation loops with a size ranging from 10 to

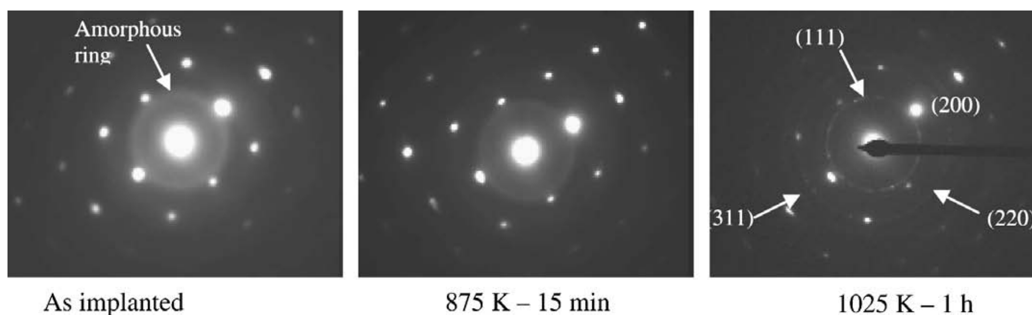

Fig. 2. Diffraction pattern evolution of Cs-implanted YSZ as a function of the annealing temperature. Non epitaxial recrystallisation is reliable with the apparition of dotted rings which correspond to the YSZ lattice parameters.

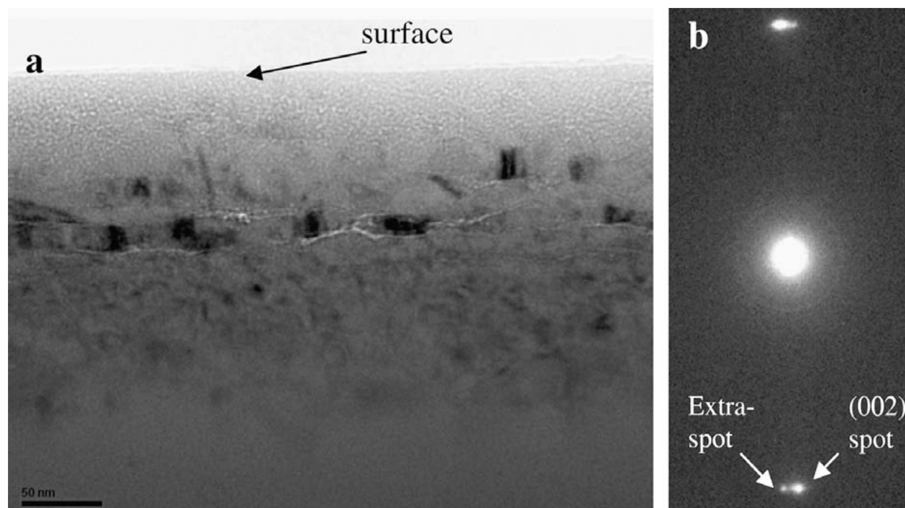

Fig. 4. (a) Off-Bragg and underfocus bright-field TEM micrograph of YSZ implanted with 300-keV Cs ions (5×10^{16} cm^{-2}) at 1025 K; and (b) SAED pattern showing extra spots related to the low-angle disorientation of grains.

20 nm. The density of dislocation loops increases with the fluence. A micrograph recorded under off-Bragg and under-focused conditions on a XTEM sample implanted with 5×10^{16} cm^{-2} (Fig. 4(a)) shows the formation of bubbles suggesting a diffusion of Cs atoms. In addition cracks are visible at about 100 nm. Amorphization is not observed at this implantation temperature but the SAED pattern exhibits extra spots (Fig. 4(b)). These extra spots are not related to additional phases but are rather associated to low-angle disoriented grains. On the off-Bragg micrograph (Fig. 4) disoriented domains are apparent with black and diffuse contrasts.

The depth distributions of Cs-implanted in YSZ, at RT and 1025 K, are plotted on Fig. 5. Up to 1×10^{16} cm^{-2} the profiles are Gaussian and are identical at both implantation temperatures. The measured maximal concentrations are in agreement with the value of 1.8 at.% calculated with the SRIM code. However at higher fluences (5×10^{16} cm^{-2}) the profiles are clearly different. At RT, the peak increases as expected, with an average discrepancy of about 20% between the measured and calculated maximal concentration, due to sputtering effects. On the contrary, at 1025 K the distribution is no longer Gaussian and the measured maximal concentration does not increase, indeed it is lower than at 1×10^{16} cm^{-2}. This depth distribution reveals a Cs saturation of about 1.5 at.% in YSZ when implanted at HT. Above this value, the increase of fluence is accompanied by a diffusion of Cs and a large release at the surface.

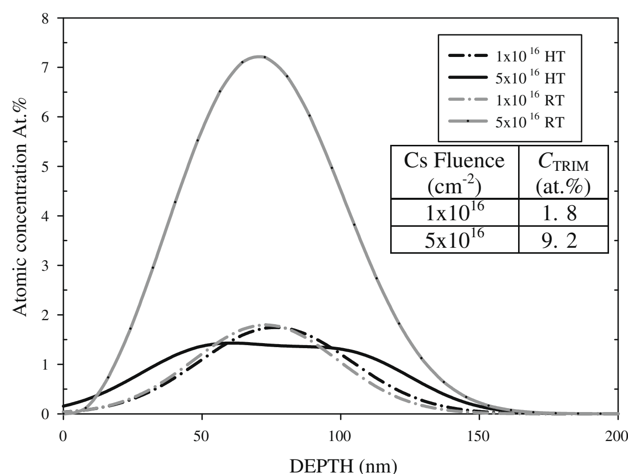

Fig. 5. Depth distribution of Cs-implanted in YSZ at 300 keV obtained from RBS spectra.

4. Discussion

Structural damage induced in YSZ by Cs ion implantation depends significantly on the irradiation temperature. A thermal contribution during implantation causes the diffusion and precipitation of point defects to develop dislocation loops. At high fluence, a dynamic recovery takes place in the form of polygonization where dislocations have been completed a rearrangement to form low-angle grain boundaries. On the contrary, at RT dislocation loops are not formed. For high Cs-concentrations, the structure undergoes a crystal-amorphous phase transformation due to a chemical effect. The static recovery of the amorphized layer after thermal annealing does not lead to polygonization but rather leaves a recovered polycrystal. Nanocrystals nucleate in the YSZ cubic structure. Diffraction patterns (Fig. 2) demonstrate that a short-range order of the initial YSZ structure is preserved in the amorphous material.

Phase predicted by Pouchon et al. [3] on the Zr–Cs–O system can not be identified on the diffraction pattern, neither after implantation, nor after thermal treatments until the final temperature studied. Previous RBS data [14] have been shown that, for crystals implanted at concentration higher than 5 at.% a release of Cs atoms occurs upon annealing above ~875 K. Thus, one can conclude that the recrystallization of the amorphous Cs rich Y-ZrO_2 is caused by the release of Cs atoms starting at 875 K. The remained concentration falls down to 1.5 at.% and no precipitation is produced contrarily to what would be expected. A thermal contribution during implantation enhances the release of Cs atoms, associated with the formation of voids and cesium zirconate precipitation does not occur. The concentration distribution displays a critical value of 1.5 at.%. This last result confirms the solubility limit of Cs in YSZ calculated by Pouchon et al. [3]. Besides, the material remains crystalline under HT implantation just because of this low retained concentration.

5. Conclusion

In as-implanted samples, the maximum Cs-concentration is about 1.5 at.% for HT implantation whereas at RT more than

7 at.% of Cs can be retained in the matrix after implantation. Under thermal annealing or implantation at 1025 K, Cs is released from YSZ. Only 1.5 at.% can be retained in solid solution. Precipitation of cesium zirconate is not observed. Post-implantation annealing leaves a recovered polycrystalline YSZ whereas thermal contribution during implantation induces polygonization.

References

[1] C. Degueldre, U. Kasermeyer, F. Botta, G. Ledergerber, Mater. Res. Soc. Symp. Proc. 412 (1996) 15.
[2] C. Degueldre, J.M. Paratte, Nucl. Technol. 123 (1998) 21.
[3] M.A. Pouchon, M. Dobeli, C. Degueldre, M. Burghartz, J. Nucl. Mater. 274 (1999) 61.
[4] L.M. Wang, S.X. Wang, R.C. Ewing, Phil. Mag. Letters 80 (2000) 341.
[5] C. Hellwig, M. Streit, P. Blair, T. Tverberg, F.C. Klaassen, R.P.C. Schram, F. Vettraino, T. Yamashita, J. Nucl. Mater. 352 (2006) 291.
[6] M. Streit, W. Wiesenack, T. Tverberg, C. Hellwig, B.C. Oberlander, J. Nucl. Mater. 352 (2006) 349.
[7] T.M. Chen, S.M. Kauzlarich, J.D. Corbett, J. Nucl. Mater. 151 (1988) 225.
[8] E.H.P. Cordfunke, R.J.M. Konings, J. Nucl. Mater. 201 (1993) 57.
[9] L. Vincent, L. Thomé, F. Garrido, O. Kaitasov, Nucl. Instrum. Method B 257 (2007) 480.
[10] L. Vincent, L. Thomé, F. Garrido, O. Kaitasov, F. Houdelier, J. Appl. Phys. 104 (2008) 114904.
[11] J.F. Ziegler, J.P. Biersack, U. Littmark, in: J.F. Ziegler (Ed.), The Stopping and Range of Ions in Solids, vol. 1, Pergamon, New York, 1985.
[12] N. Chauvin, S. Henry, H. Flocard, F. Fortuna, O. Kaitasov, P. Pariset, S. Pellegrino, M.O. Ruault, Y. Serruys, P. Trocellier, Nucl. Instrum. Meth. B261 (2007) 34.
[13] A. Guinier, Théorie et Technique de la Radiocristallographie, Dunod, Paris, 1964. p. 452.
[14] L. Thomé, A. Gentils, S.E. Enescu, H. Khodja, T. Thomé, Nucl. Instrum. Meth. B 249 (2006) 326.